Physica Medica 57 (2019) 1–6

Contents lists available at ScienceDirect

Physica Medica

journal homepage: www.elsevier.com/locate/ejmp

Original paper

Investigation of shutter scan acquisition parameters in a prototype chest digital tomosynthesis system

Dohyeon Kim[a], Donghoon Lee[a], Haenghwa Lee[b], Hyemi Kim[b], Zhen Chao[a], Minjae Lee[a], Hee-Joung Kim[a,b,*]

[a] Department of Radiation Convergence Engineering, Research Institute of Health Science, Yonsei University, 1 Yonseidae-gil, Wonju, Gangwon 220-710, Republic of Korea
[b] Department of Radiological Science, College of Health Science, Yonsei University, 1 Yonseidae-gil, Wonju, Gangwon 220-710, Republic of Korea

ARTICLE INFO

Keywords:
Digital tomosynthesis
Dose reduction method
Region of interest reconstruction
Shutter scan acquisition

ABSTRACT

A shutter scan acquisition (SSA) method is proposed to reduce patient exposure dose in a chest digital tomosynthesis system. Projections obtained using the SSA constitute a combination of truncated and non-truncated projections. The truncated projections are images in which the lung field is set within a region-of-interest (ROI), and the non-truncated projections are full images in which the ROI is not set at all. We proposed a shutter weighting factor (SWF) as an acquisition parameter for SSA. We call the number of truncated projections divided by the number of non-truncated projections as SWF. We used a prototype CDT system and the LUNGMAN phantom with 8 and 10 mm lung nodules. 81 projections were obtained using SSA in five sets according to the SWFs. The image quality was quantified based on the contrast-to-noise ratio (CNR). We also calculated the figure of merit (FOM) to determine the proper acquisition parameters of the five sets. Both the CNR and FOM values of the 8 mm lung nodule in the selected ROI increased with increases of the SWF. However, the CNR value of the 10 mm lung nodule outside the ROI decreased with increases of the SWF, while the FOM value was maximized when the SWF was 3.05. We investigated the effect of the composition ratio of the truncated and non-truncated projections on the reconstructed images of the SSA based on the FOM values. In conclusion, we determined the proper SSA parameters in a prototype CDT system.

1. Introduction

Low dose imaging techniques are of great interest in medical applications. Correspondingly, digital tomosynthesis systems have been studied to reduce the patient exposure dose. Nevertheless, many studies have suggested that reductions in the exposure dose in digital tomosynthesis systems are still required. Diagnostically important information is often concentrated in a region of interest (ROI) in a reconstructed 3D image. For this reason, ROI imaging techniques are considered to be an effective dose reduction method. If the ROI reconstruction method is applied to a digital tomosynthesis system, better dose reduction effects are expected.

The conventional ROI imaging method can reconstruct only interior ROIs [1,2]. ROI imaging is a technique for obtaining only the image of the area to be diagnosed by limiting the FOV using the x-ray collimator. ROI imaging techniques have been mainly studied in computed tomography (CT) and digital tomosynthesis systems. For example, Zhang et al. (2016) reported the study of ROI reconstruction using a two-step filtering-based iterative image reconstruction algorithm [3]. Park et al. (2017) reported the ROI reconstruction method for a digital tomosynthesis system using scout view information to improve the reconstructed ROI images [4]. All studies suggest that limiting the field of view (FOV) can improve the internal image quality of the ROI and reduce the patient exposure so that the ROI reconstruction is suitable for clinical applications. Although many studies have been performed on ROI imaging in various medical applications, most of them have not focused on the improvements of the image quality of the overall anatomy outside the ROI [5]. To solve this problem, we have reported a shutter scan acquisition (SSA) method based on ROI imaging in a digital tomosynthesis system [6]. SSA is a method that entails opening the X-ray collimator during ROI imaging for including external information to the ROI. Thus, the obtained projections consist of truncated (collimated) and non-truncated (non-collimated) projections. The difference between the proposed SSA and ROI imaging is that the image contrast of the ROI can be enhanced, and the information outside the ROI can be obtained.

* Corresponding author at: Department of Radiation Convergence Engineering, Research Institute of Health Science, Yonsei University, 1 Yonseidae-gil, Wonju, Gangwon 220-710, Republic of Korea.
E-mail address: hjk1@yonsei.ac.kr (H.-J. Kim).

https://doi.org/10.1016/j.ejmp.2018.12.004
Received 27 March 2018; Received in revised form 15 November 2018; Accepted 8 December 2018
Available online 12 December 2018

Fig. 1. (a) Prototype chest digital tomosynthesis system, (b) lung nodule and LUNGMAN phantom, and (c) the location of the lung nodules.

Table 1
Specifications of the prototype chest digital tomosynthesis system.

SDD	SOD	Reconstruction method	Detector pixel size	Number of projections (angle interval)	X-ray exposure condition
1000–1500 mm	900–1400 mm	FBP	1440 × 1440	81 (0.5°)	1.1 mm Al at 100 kVp 100 mA, 10 ms (for each projection)

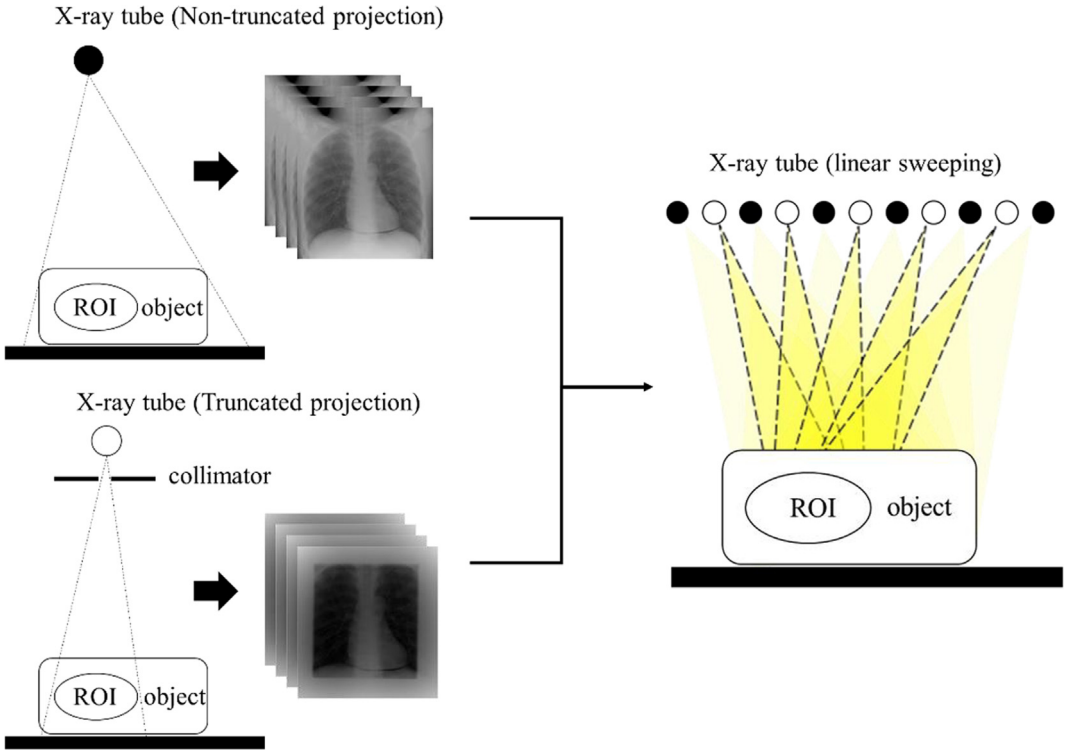

Fig. 2. Illustration of the shutter scan acquisition in the digital tomosynthesis system.

In our previous study, we demonstrated that the proposed SSA can be applied to a digital tomosynthesis system [6]. The result of previous study has confirmed the possibility of SSA method and verified proposed image processing method for truncation artifact. However, we have not yet investigated how the ratio of truncated projection and non-truncated projections can be set when the proposed SSA is applied to clinical practice. The quality of the image and efficiency of dose reduction can vary owing to the composition ratio of the truncated and non-truncated projections. Investigation of acquisition parameters is indispensable for practical clinical applications [7]. We believe that an optimization study of the acquisition parameter composition ratio is necessary for the SSA method. We proposed an acquisition parameter called a shutter weighting factor (SWF) and evaluated how the image quality varies according to the SWF. Based on these results, we determined the most proper acquisition parameter for the SSA method.

In this study, we applied the SSA to a prototype chest digital tomosynthesis system and evaluated the quality of the reconstructed image. The purpose of this study was to investigate the effect of the composition ratio of the truncated and non-truncated projections and to determine a proper set of acquisition parameters for the proposed SSA in digital tomosynthesis systems among the 5 acquisition sets.

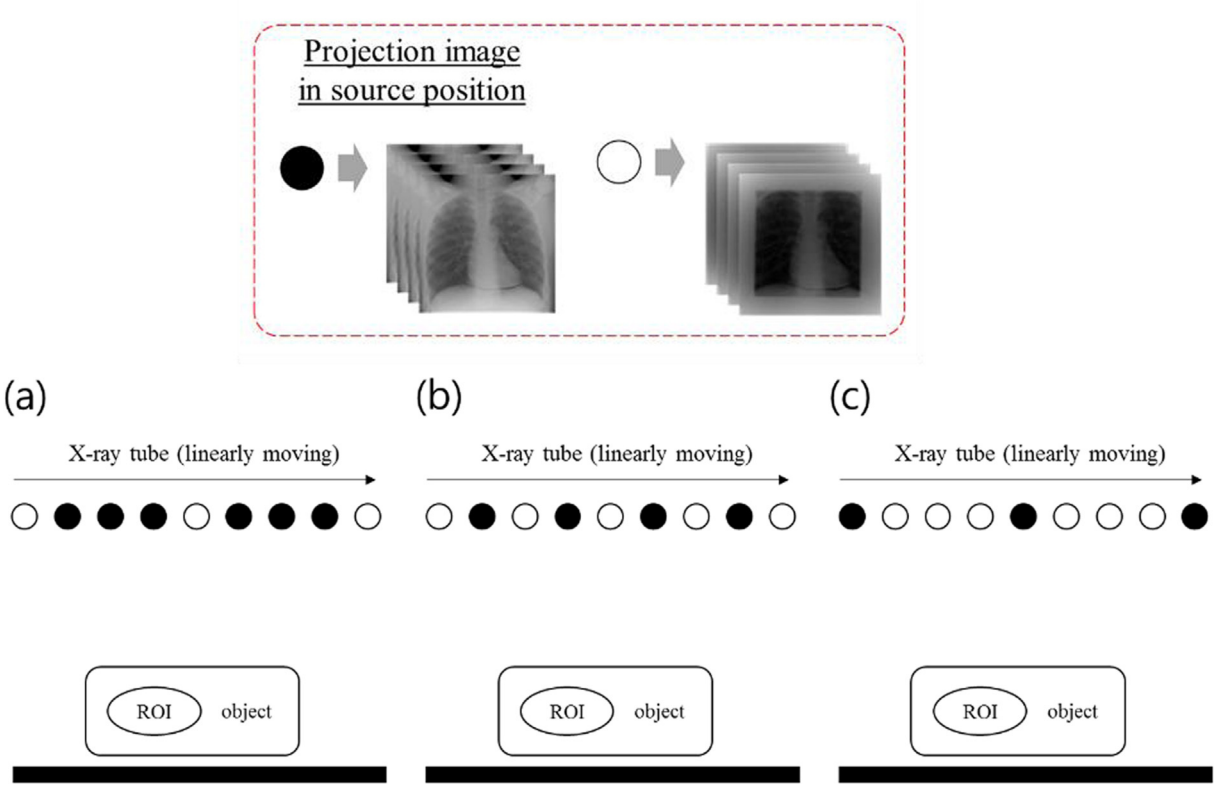

Fig. 3. Illustration of projection distribution according to the shutter weighting factor: (a) SWF < 1.03, (b) SWF = 1.03, (c) SWF > 1.03.

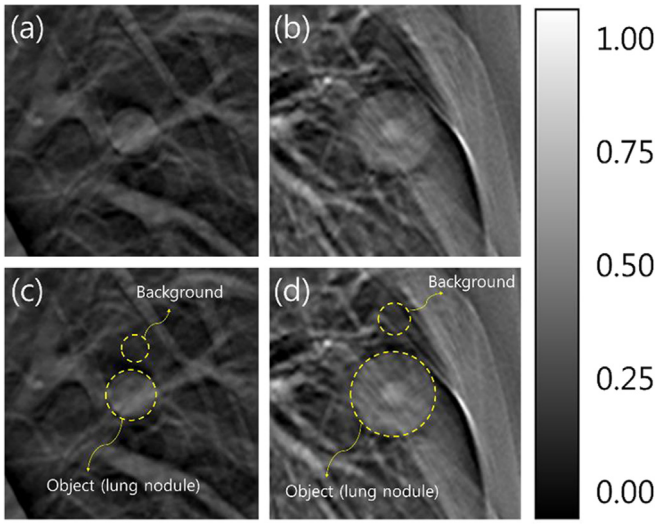

Fig. 4. ROI settings in the reconstructed images for CNR evaluation: (a) reconstructed image of enlarged 8 mm lung nodule, (b) reconstructed image of enlarged 10 mm lung nodule, (c) reconstructed image of enlarged 8 mm lung nodule (ROI setting), (d) reconstructed image of enlarged 10 mm lung nodule (ROI setting).

2. Materials and methods

2.1. Experimental set-up

We used a prototype chest digital tomosynthesis (CDT) system (LISTEM, Wonju, Korea). This system is still at a developmental stage, and is undergoing preparation for the potential clinical applications in Wonju Sevrance Christian Hospital (Wonju, Korea). The system consists of a CsI(Tl) scintillator flat panel detector (Pixium RF 4343, Thales, France), X-ray tube (E7869X, Toshiba), a main controller, and reconstruction server. The source-to-detector distance (SDD) and the source-to-object distance (SOD) were 1100 and 1000 mm, respectively. The X-ray tube moved linearly at a speed of 160 mm/s while rotating from −20° to 20° with a 0.5° angle step for 81 projections. The phantom used in this study was a multipurpose chest phantom (LUNGMAN, Kagaku, Japan) with a normal anatomical structure of the human chest and lung nodules of 8 and 10 mm. The phantom is made based on the chest torso of an adult male and weighs about 18 kg. A photograph of the prototype CDT system and a LUNGMAN phantom with a lung nodule are shown in Fig. 1. The 8 mm lung nodule is a standard type with only one substance inside. The 10 mm lung nodule is a GGO concentric type, and its internal structure consists of a GGO field and a solid field. Table 1 lists the major acquisition parameters of the prototype CDT system. Obtained projections were reconstructed by a filtered back projection (FBP) algorithm. The reconstructed image had a volume of 1000 × 1000 × 50 voxels.

Projections obtained by SSA consisted of truncated and non-truncated projections. If the number of truncated projections was 71, 10 non-truncated projections were obtained at regular angle interval. The truncated projections were images in which the lung field was set within the region of interest (ROI) by using a collimation system, and the non-truncated projections are full images. Part of the projections obtained by the proposed SSA method are truncated. Truncation artifacts in reconstructed images can be caused by the truncated portion of the projections. Therefore, an image processing procedure is required for the SSA method [6]. The illustration of the SSA is presented in Fig. 2. We defined the number of truncated projections divided by the number of non-truncated projections as the SWF. The SSA parameters were optimized using 5 acquisition sets with the SWFs of 0.16, 0.35, 1.03, 3.05, and 7.1. The distribution of truncated and non-truncated projections can be explained in three cases as shown in the Fig. 3. When the shutter weighting factor is smaller than 1.03, truncated projections are distributed at regular angular intervals as shown in Fig. 3(a), and then the remaining non-truncated projections are distributed. When the

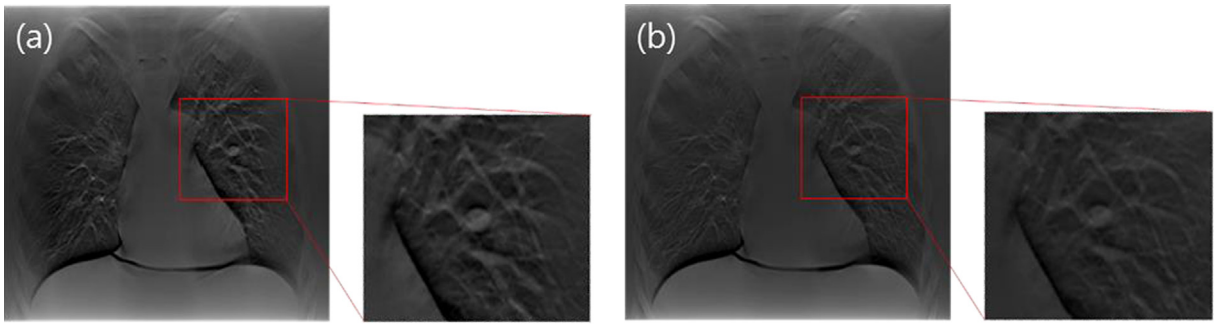

Fig. 5. Reconstructed images of the LUNGMAN phantom: (a) shutter scan and (b) conventional full view acquisition.

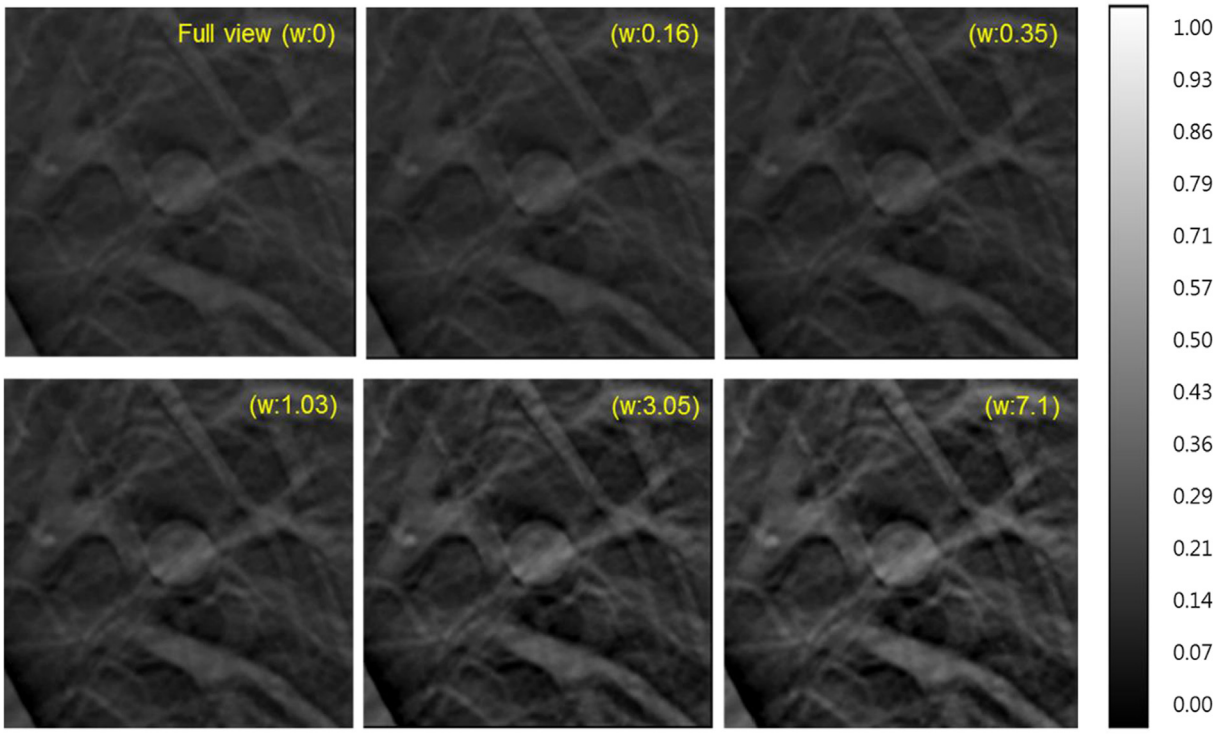

Fig. 6. Enlarged 8 mm lung nodule (within the ROI) in the reconstructed images using 5 acquisition sets.

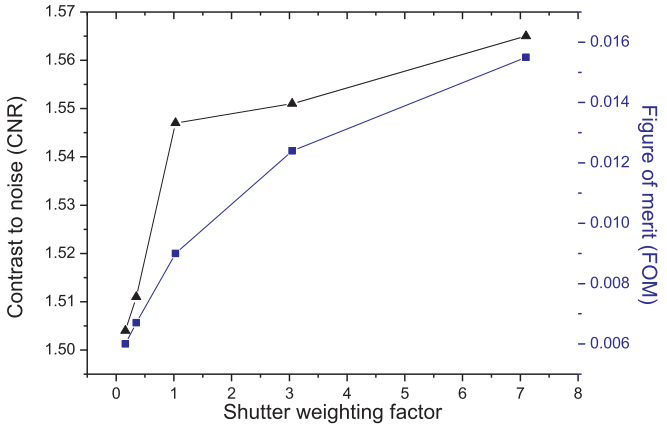

Fig. 7. Changes in the CNR and FOM values of the 8 mm lung nodule within the ROI.

shutter weighting factor is 1.03, both truncated projections and non-truncated projections are distributed at regular angular intervals as shown in Fig. 3(b). When the shutter weighting factor is larger than 1.03, the non-truncated projections are distributed at regular angular intervals as shown in Fig. 3(c), and then the remaining truncated projections are distributed. The SWF can be expressed as follows,

$$\text{Shutter weighting factor} = \frac{number\ of\ truncated\ projections}{number\ of\ non-truncated\ projections}$$

2.2. Quantitative evaluation

We evaluated the contrast enhancement and dose reduction effect using the contrast to noise ratio (CNR) and figure of merit (FOM). Proper acquisition parameters were determined from the calculated FOM value for the SSA. We set the ROIs and background on each slice, with the ROIs positioned to include the 8 and 10 mm lung nodules, as presented in Fig. 4. First, the CNR values of the lung nodules were calculated based on the following equation:

$$\text{CNR} = \frac{|S_{object} - S_{background}|}{\sqrt{({\sigma_{object}}^2 + {\sigma_{background}}^2)}}$$

where S_{object} and$S_{background}$ are the mean values, and σ_{object} and$\sigma_{background}$ are the standard deviations of the object and background regions, respectively.

Table 2
Results of CNR, effective dose and FOM analysis, in the case of 8 mm lung nodule.

Shutter weighting factor	CNR	Effective dose (μSv)	FOM	Normalized FOM
0.16	1.504	380.0	0.0060	0
0.35	1.511	328.9	0.0069	0.09
1.03	1.547	265.9	0.0090	0.32
3.05	1.551	194.0	0.0124	0.67
7.1	1.565	158.0	0.0155	1

In addition, the FOM values of the lung nodules were calculated to quantitatively evaluate the image quality compared to the exposure dose.

The FOM values were calculated based on the following equation [8],

$$\text{FOM} = \frac{\text{CNR}^2}{\text{effective dose}}$$

The total effective dose was used as the dose value required to calculate the FOM. We estimated the effective patient dose in the digital tomosynthesis system using the PCXMC 2.0 software (STUK, Helsinki, Finland), that simulated the effective dose based on a Monte Carlo simulation in association with publication 103 of the ICRP [9,10]. We simulated the geometry according to 5 sets of SSA parameters. Simulation was performed considering the acquisition condition such as the X-ray tube angulation. This software tool calculated the organ dose in 11 organs which were located in the chest field. 2.0×10^5 photons were used for each of the 81 projections of the tomosynthesis acquisition, thus resulting in a total of 1.62×10^7 photons for the entire acquisition. In the simulation, the effective dose was measured for a typical patient weighting 65 kg with a height of 175 cm based on existing data for an average adult male.

3. Results

Fig. 5 shows the results of comparing the reconstructed images obtained by the shutter scan (SWF: 1.03) and the conventional full view scan in the 37th slice. The ROI of the reconstructed image with SSA yielded an enhanced contrast, as shown in Fig. 5. Projections were acquired according to various acquisition parameters to optimize the image quality compared to the exposure dose.

Fig. 6 shows the results of an enlarged 8 mm lung nodule image within the ROI, obtained according to the various SWFs. Both the CNR and FOM values of the 8 mm lung nodule in the ROI increased as the SWF increased. Fig. 7 and Table 2 show the CNR, effective dose, and FOM values. Both the CNR and FOM values increased in proportion to the SWF. The highest CNR and FOM values were elicited for a SWF of 7.1, which was obtained for the acquisition set that consisted of 71 truncated projections and 10 non-truncated projections. Fig. 8 shows the results of the enlarged 10 mm lung nodule image obtained outside the ROI for various SWFs. Fig. 9 and Table 3 show CNR, effective dose, and FOM values. The CNR value decreased as the SWF increased. The highest FOM value was obtained for the acquisition set that consisted of 61 truncated projections and 20 non-truncated projections with a SWF of 3.05.

4. Discussion

Reconstructed images were successfully acquired by applying the proposed SSA method. Reconstructed images obtained by the SSA method contain the entire set of anatomical information. Because projection data obtained by the SSA contains the ROI's external information, the entire anatomical information can be restored in the reconstructed image. This can be a great help in establishing an accurate diagnosis and treatment plan. In this study, we proposed an acquisition parameter referred to as SWF and contributed to the evaluation of the image quality and dose to define the most appropriate acquisition parameters.

The results demonstrate that CNR of the lung nodule within the ROI increases as the weighting factor increases. The reason for the increase

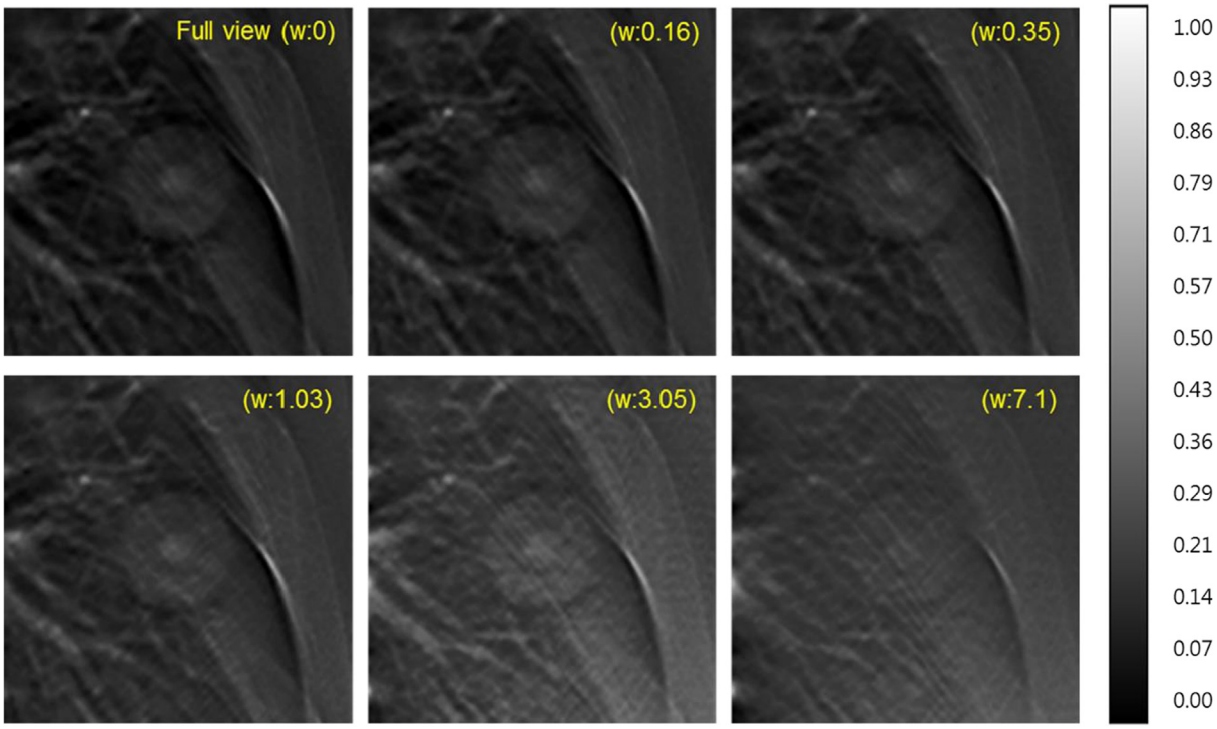

Fig. 8. Enlarged 10 mm lung nodule (outside the ROI) in the reconstructed images using 5 acquisition sets.

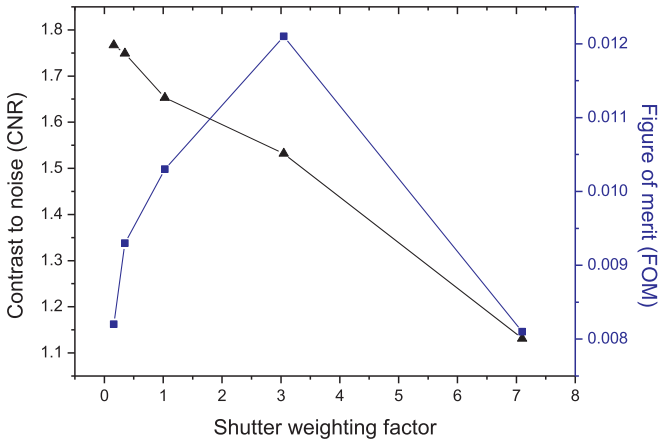

Fig. 9. Changes in the CNR and FOM values of the 10 mm lung nodule outside the ROI.

Table 3
Results of CNR, effective dose and FOM analysis of the 10 mm lung nodule.

Shutter weighting factor	CNR	Effective dose (μSv)	FOM	Normalized FOM
0.16	1.767	380.0	0.0082	0.03
0.35	1.749	328.9	0.0093	0.3
1.03	1.653	265.9	0.0103	0.55
3.05	1.532	194.0	0.0121	1
7.1	1.131	158.0	0.0081	0

of the CNR value is attributed to the fact that the amount of scattered radiation into the ROI decreased. When the truncated projection was acquired, the amount of scattered radiation that reached the detector decreased as the field of view size decreased [11,12]. As the SWF increased, the number of truncated projections increased. However, further studies are needed to determine the amount of scattered radiation as the field of view size decreases. The value of the lung nodule of CNR within the ROI increased as the SWF increased. However, the value of the CNR of the lung nodules outside the ROI decreased. The CNR value of the lung nodules outside the ROI was inevitably decreased because the external information in the ROI was insufficient as the SWF increased. When the SWF is increased, CNR reduction of the 10 mm lung nodule outside the ROI is larger than the CNR increase of the 8 mm lung nodule inside the ROI. The CNR of the 8 mm lung nodule within the ROI do not suffer external information loss according to the SWF. However, the 10 mm lung nodule outside the ROI is expected to have a large degree of CNR reduction because the loss of external information is increased due to the increase of the SWF.

As the FOM value is a factor that indicates the quality of the image relative to the patient's exposure dose, it can be a useful factor for presenting the proper acquisition parameters [13,14]. The FOM value is affected by the change of the CNR value and the change of the effective dose. As the SWF increases, the effective dose generally decreases and the CNR value increases or decreases depending on the position of the lung nodule under evaluation. When we diagnose a lesion that is present within the ROI, a higher SWF is better for the SSA because the FOM values continue to increase as a function of the SWF. However, when we need to diagnose a lesion outside the ROI, the optimal image can be obtained under the acquisition condition with the SWF of 3.05, as presented in this study. For clinically effective diagnosis, it is necessary to determine the proper acquisition parameters according to proposed SWF.

As can be seen from the results of this study, proposed SWF can define the proper acquisition parameter in the clinic by changing the ratio of truncated projection to non-truncated projection. When the SSA method is applied to the clinic, it is necessary to determine the acquisition parameter according to the diagnostic situation by calculating the SWF because the image quality compared to the exposure dose is varied as the result of this study. Therefore, in order to apply the SSA method to clinical practice, many further studies using a SWF to define proper acquisition parameters are expected to be conducted.

The SSA was useful when the selected ROI within a patient's body was small, and when its location was known (such as the heart, teeth, or lung field), because the SSA focused on obtaining a full image with an enhanced ROI. The SSA method can be used when external information needs to be considered together for diagnosis and treatment planning. The proposed SSA can also obtain images with improved contrast compared to the dose so that increased diagnostic value can be expected in a digital tomosynthesis system. Obtaining a high-contrast image has a high-diagnostic value because it makes it easier to distinguish lesions and normal tissue.

5. Conclusion

In conclusion, we applied the SSA method to the prototype CDT system under development, and proposed a SWF as the SSA parameter. We investigated the effect of the composition ratio of the truncated and non-truncated projections on the reconstructed images through the SSA. Proper SSA parameters were determined by deriving the FOM values among the 5 acquisition sets. Our results suggest possible directions for further improvements in digital tomosynthesis systems for the SSA method.

Acknowledgement

This research was financially supported by the Ministry of Trade, Industry, and Energy (MOTIE), the Korea Institute for Advancement of Technology (KIAT), and the Gangwon Institute for Regional Program Evaluation (GWIRPE) through the Encouragement Program for The Industries of Economic Cooperation Region (No. R0002898). Also, this research was supported by Basic Science Research Program through the National Research Foundation of Korea (NRF) funded by the Ministry of Science, ICT & Future Planning (NRF-2017R1A2B2001818).

References

[1] Wang G, Yu H. The meaning of interior tomography. Phys Med Biol 2013;58(16):R162–86.
[2] Ward JP, Lee M, Ye JC, Unser M. Interior tomography using 1D generalized total variation-part I: mathematical foundation. SIAM J Imaging Sci 2015;8(1):226–47.
[3] Zhang H, Li L, Yan B, Wang L, Cai A, Hu G. A two-step filtering-based iterative image reconstruction method for interior tomography. J X-ray Sci and Technol 2016;24(5):733–47.
[4] Park S. Scout-view assisted interior digital tomosynthesis (iDTS) based on compressed-sensing theory. Radiat Phys and Chem 2017;141:29–35.
[5] Lee J. Improving image accuracy of region-of-interest in cone-beam CT using prior image. J Appl Clin Med Phys 2014;15(2). https://doi.org/10.1007/978-3-642-29305-4_276.
[6] Kim D. Feasibility study of shutter scan acquisition for region of interest (ROI) digital tomosynthesis. J Appl Clin Med Phys 2018;19(2). https://doi.org/10.1002/acm2.12294.
[7] Lee H. Investigation of various reconstruction parameters for algebraic reconstruction technique in a newly developed chest digital tomosynthesis. J Instrumentation 2017;12:P08016.
[8] Gislason-Lee AJ. Dose optimization in cardiac X-ray imaging. Med Phys 2013;40(9). https://doi.org/10.1118/1.4818016.
[9] Tapiovaara M, Lakkisto M, Servomaa A PCXMC: a PC-based Monte Carlo program for calculating patient doses in medical X-ray examinations, Finland, STUK–A, 1997:139.
[10] Sabol JM. A Monte Carlo estimation of effective dose in chest tomosynthesis. Med Phys 2009;36(12):5480–7.
[11] Chityala R, Hoffmann KR, Rudin S, Bednarek DR. Region of interest (ROI) computed tomography (CT): comparison with full field of view (FFOV) and truncated CT for a human head phantom, in: Medical Imaging 2005: Phys Med Imaging 2005; 5745(1): 583–590, International Society for Optics and Photonics.
[12] Sprawls P. The physical principles of medical imaging (scattered radiation and contrast). http://www.sprawls.org/ppmi2/SCATRAD (accessed 13 March 2018).
[13] Maldera A, De Marco P, Colombo PE, Origgi D, Torresin A. Digital breast tomosynthesis: dose and image quality assessment. Phys Medica 2017;33:56–67.
[14] Di Maria S, Baptista M, Felix M, Oliveira N, Matela N, Janeiro L, et al. Optimal photon energy comparison between digital breast tomosynthesis and mammography: a case study. Phys Medica 2014;30(4):482–8.